Conditional Panoramic Image Generation via Masked Autoregressive Modeling

Chaoyang Wang[1] **Xiangtai Li**[1] **Lu Qi**[2*] **Xiaofan Lin**[2]
Jinbin Bai[3] **Qianyu Zhou**[4] **Yunhai Tong**[1]
[1]School of Intelligence Science and Technology, Peking University
[2]Insta360 Research [3]National University of Singapore [4]The University of Tokyo
cywang@stu.pku.edu.cn, qqlu1992@gmail.com

Figure 1: **Generated samples from Panoramic AutoRegressive (PAR) Model**. PAR unifies several conditional panoramic image generation tasks, including text-to-panorama, panorama outpainting, and panoramic image editing.

Abstract

Recent progress in panoramic image generation has underscored two critical limitations in existing approaches. First, most methods are built upon diffusion models, which are inherently ill-suited for equirectangular projection (ERP) panoramas due to the violation of the identically and independently distributed (*i.i.d.*) Gaussian noise assumption caused by their spherical mapping. Second, these methods often treat text-conditioned generation (text-to-panorama) and image-conditioned generation (panorama outpainting) as separate tasks, relying on distinct architectures and task-specific data. In this work, we propose a unified framework, Panoramic AutoRegressive model (PAR), which leverages masked autoregressive modeling to address these challenges. PAR avoids the *i.i.d.* assumption constraint and integrates text and image conditioning into a cohesive architecture, enabling seamless generation across tasks. To address the inherent discontinuity in existing generative models, we introduce circular padding

*Corresponding author

39th Conference on Neural Information Processing Systems (NeurIPS 2025).

to enhance spatial coherence and propose a consistency alignment strategy to improve the generation quality. Extensive experiments demonstrate competitive performance in text-to-image generation and panorama outpainting tasks while showcasing promising scalability and generalization capabilities. Project Page: https://wang-chaoyang.github.io/project/par.

1 Introduction

Panoramic image generation[2, 12, 13, 18, 19] has recently emerged as a pivotal research direction in computer vision, driven by its capability to capture immersive 360-degree horizontal and 180-degree vertical fields of view (FoV). This unique visual representation closely mimics human panoramic perception, enabling transformative applications across VR/AR [34, 79], autonomous driving [44], visual navigation [6, 25], and robotics [45, 60].

Despite some progress in recent years, existing panorama generation methods [18, 56, 57, 74, 70, 27, 36, 62, 77, 65, 64, 76] predominantly rely on diffusion-based base models and face two significant problems: task separation and inherent limitations of the modeling approach. First, different panoramic generation tasks are highly bound to specific foundation models. For instance, most text-to-panorama models [18, 56, 57, 74, 70] are based on Stable Diffusion (SD) [48, 43]. In contrast, panorama outpainting models [27, 36, 62] are fine-tuned on SD-inpainting variants, resulting in task-specific pipelines that lack flexibility. Second, diffusion-based models struggle to handle the unique characteristics of equirectangular projection (ERP) panoramas, which map spherical data onto a 2D plane, violating the *i.i.d.* Gaussian noise assumption.

In addition to these fundamental issues, existing methods also contain redundant modeling, which introduces unnecessary computational costs. This redundancy manifests in several ways: 1) Some approaches [29, 36] iteratively inpaint and warp local areas, leading to error accumulation over successive steps. 2) Others [74, 55] adopt a dual-branch structure, with global and local branches, where the local branches are not directly used as final output targets. These challenges underscore the need for a straightforward, unified, and efficient paradigm for generating conditional panoramic images.

In this work, we explore a powerful yet less explored panoramic image generation paradigm to address the above limitations: the violation of the *i.i.d.* assumption and the lack of unification. Moreover, we allow the model to take text or images as input and control the generated content at any position on the canvas. As shown in Fig. 1, PAR is competent for text-to-panorama, panorama outpainting, and editing tasks. Notably, our PAR requires no task-specific data engineering - both conditions are seamlessly integrated via a single likelihood objective. In comparison, Omni^2 [68] relies on meticulously designed joint training datasets to align heterogeneous tasks, inevitably introducing complexity and domain bias.

For this goal, inspired by masked autoregressive modeling (MAR) [30], we propose PAR. On the one hand, it is based on AR modeling, which avoids the constraints of *i.i.d.* assumptions. On the other hand, it allows for generation in arbitrary order, overcoming the shortcoming of traditional raster-scan methods that are incapable of image-condition generation. This flexibility of PAR unifies conditional generation tasks - panorama outpainting reduces to a subset of text-to-panorama synthesis, where existing image tokens serve as partially observed sequences. Building upon the MAR-based generative framework, we introduce two critical enhancements to address inherent limitations in standard architectures. First, conventional VAE-based compression often exhibits spatial bias during encoding-decoding: center regions benefit from contextual information across all directions, while peripheral pixels suffer from unidirectional receptive fields, contradicting the cyclic nature of ERP panoramas. To mitigate this, we propose *dual-space circular padding*, applying cyclic padding operations in both latent and pixel spaces. This ensures seamless feature propagation across ERP boundaries, aligning geometric and semantic continuity. Second, as the foundation model is pre-trained on massive perspective images, we devise a *translation consistency loss*. This loss explicitly regularizes the model to accommodate the prior of ERP panoramas by minimizing discrepancies between the model's outputs under shifted and original inputs. Ultimately, two innovations holistically reconcile the unique demands of 360-degree imagery with the flexibility of MAR modeling. Experiments demonstrate that PAR outperforms specialist models in the text-to-panorama task, with 37.37 FID on the Matterport3D dataset. Moreover, on the outpainting task,

it has better generation quality and avoids the problem of repeated structure generation. Ablation studies demonstrate the model's scalability in terms of computational cost and parameters, as well as its generalization to out-of-distribution (OOD) data and other tasks, such as zero-shot image editing.

Our contribution can be summarized as follows: 1) We propose PAR, which fundamentally avoids the conflict between ERP and *i.i.d.* assumption raised by diffusion models, and also seamlessly integrates text and image-conditioned generation within a single architecture. 2) To enforce better adaptation to the panorama characteristic, we propose specialized designs, including dual-space circular padding and a translation consistency loss. 3) We evaluate our model on popular benchmarks, demonstrating competitive performance in text and image-conditional panoramic image generation tasks. The results also prove the scalability and generalization capabilities of our model.

2 Related Work

Conditional Panoramic Image Generation. There are two primary task paradigms in this area: 1) text-to-panorama (T2P), which synthesizes 360-degree scenes from textual descriptions, and 2) panorama outpainting (PO), which extends partial visual inputs to full panoramas. Given the success of diffusion models (DMs) [31, 32, 33, 43, 48, 51, 52] on generation tasks, such as image generation [48, 75, 23, 43, 42, 17], image editing [4, 37, 49], image super resolution [22, 50, 71], video generation [3, 20, 69], current approaches typically build upon DMs, yet face two problems. First, DM is inherently unsuitable for panorama tasks due to reliance on the *i.i.d.* Gaussian noise assumption, which ERP transformations violate. Second, existing approaches lack task unification. Specifically, T2P methods typically fine-tune SD, while PO solutions adapt the SD-inpainting variants. Although some work [68] attempts a unified solution, it is based on DM and relies on complex task-specific data engineering. From a methodological perspective, existing methods can be categorized into two main approaches: bottom-up and top-down. The former generates images with limited FoV sequentially [29, 36] or simultaneously [57, 27] and finally stitches them together, but faces the problem of lacking global information and error accumulation. The latter [74, 55] typically employs a dual-branch architecture comprising a panorama branch and a perspective branch. However, this design brings unnecessary computational cost. In parallel, several AR-based attempts have been made. They either rely on large DMs for final generation [36, 19], are limited to low resolution with additional up-sampling modules [10], or stitch perspective images without correct panorama geometry [80]. Overall, existing methods do not provide a unified and theoretically sound solution for conditional panorama generation, which we rethink through MAR modeling.

Autoregressive Modeling. Motivated by the success of large language models (LLMs) [5, 58], AR models, with great scalability and generalizability, are becoming a strong challenger to diffusion models. Several studies delve into visual AR with two distinct pipelines. One pipeline adopts raster-scan modeling [53, 47, 15, 16, 72, 63, 67, 28, 39], which treats the image as visual sentences and sequentially predicts the next token. However, this strategy does not fully exploit the spatial relationships of images. To make up for the shortcomings of raster-scan modeling, some works [7, 24, 73, 59, 30, 14, 1] extend the concept of masked generative models [8] to AR modeling, namely MAR. Instead of predicting one token within one forward, the model randomly selects several candidate positions and predicts attending to the decoded positions. Intuitively, this modeling provides flexible control over arbitrary spatial positions simply by adjusting the order of tokens to be decoded. Hence, we resort to MAR as a flexible way to unify text and image-conditioned panorama generation while avoiding the theoretical defects of panorama DMs.

3 Method

This section is organized into three parts. First, we introduce the preliminaries of panorama projection and review the standard conditional AR modeling. Second, we analyze the disadvantages of this approach for unified conditional generation. Last, we describe our PAR in the following sections, including vanilla MAR architecture, consistency alignment, and circular padding.

3.1 Preliminaries

Equirectangular Projection is a common parameterization for panoramic images. It establishes a bijection between spherical coordinates (θ, ϕ) and 2D image coordinates (u, v), where $\theta \in [0, \pi]$

denotes the polar angle (latitude) and $\phi \in (-\pi, \pi]$ represents the azimuthal angle (longitude). This projection preserves complete spherical visual information while maintaining compatibility with conventional 2D convolutional operations. Given a 3D point $\mathbf{P} = (x, y, z)$ on the unit sphere $\mathbb{S}^2$, we first compute its spherical coordinates and then obtain ERP coordinates (u, v) via linear mapping:

$$\phi = \arctan\left(\frac{y}{x}\right), \quad \theta = \arccos(z), \quad u = \frac{\phi + \pi}{2\pi} W, \quad v = \frac{\theta}{\pi} H, \tag{1}$$

where $W \times H$ denotes the target image resolution.

Conditional Autoregressive Models formulate conditional data generation as a sequential process through next token prediction. Given an ordered sequence of tokens $\{x_t\}_{t=1}^{T}$, the joint distribution $p(x|c)$ factorizes into a product of conditional probabilities:

$$p(x|c) = \prod_{t=1}^{T} p(x_t|x_{<t}, c), \tag{2}$$

where $x_{<t} \equiv (x_1, ..., x_{t-1})$ denotes the historical context and c indicates the conditions. This chain rule decomposition enables tractable maximum likelihood estimation, with the model parameters θ optimized to maximize:

$$\mathcal{L}(\theta) = \mathbb{E}_{x \sim \mathcal{D}} \left[\sum_{t=1}^{T} \log p_\theta(x_t|x_{<t}, c) \right], \tag{3}$$

where $\mathcal{D}$ represents the data distribution.

3.2 Rethinking Conditional Panoramic Image Generation

While DMs have demonstrated remarkable success in various image generation tasks, they rely on *i.i.d.* Gaussian noise assumption, which is violated by the spatial distortions introduced by the ERP transformation in Eq. 1, making diffusion-based methods inherently unsuitable for modeling panoramas. In this work, we therefore rethink conditional panorama generation from AR modeling, which is not constrained by such assumptions.

Building upon the standard conditional AR formulation in Eq. 2, we analyze text-to-panorama and panorama outpainting scenarios. The former takes text embeddings as c while the latter takes observed image patches and optional textual prompts as conditions. In particular, this reformulates the two problems as follows:

$$p(x|c) = \prod_{t \in \mathcal{S}_u} p(x_t|x_{\mathcal{S}(t)}, c), \quad \mathcal{S}(t) \subseteq (\mathcal{S}_k \cup \{1, ..., t-1\}), \tag{4}$$

where $\mathcal{S}_k$ denotes known token positions from the condition and $\mathcal{S}_u = \{1, ..., T\} \setminus \mathcal{S}_k$ are targets. The context set $\mathcal{S}(t)$ dynamically aggregates:

$$\mathcal{S}(t) = \underbrace{\{j|j \in \mathcal{S}_k\}}_{\text{condition}} \cup \underbrace{\{j|j < t, j \in \mathcal{S}_u\}}_{\text{generated content}}, \tag{5}$$

This formulation generalizes text-to-panorama ($\mathcal{S}_k = \emptyset$) and outpainting ($\mathcal{S}_k \neq \emptyset$) scenarios. However, traditional raster-scan modeling is not competent for the panorama outpainting task, as $\mathcal{S}_k$ is not necessarily at the beginning of the sequence.

3.3 Masked Autoregressive Modeling with Consistency Alignment

We aim to learn a generalized AR model that naturally unifies text and image conditions and adapts to panoramic characteristics. An intuitive solution is MAR modeling, which allows generation in arbitrary order by marking the position of each token. However, existing foundation models are typically pre-trained on perspective images and cannot cope with panoramic scenarios. We delve into this problem and use the cyclic translation equivariance of ERP panoramas.

Vanilla Architecture. We start with a vanilla text-conditioned MAR model [14] to learn basic image generation without special constraints. Specifically, we use continuous tokens instead of discrete ones to reduce quantization error.

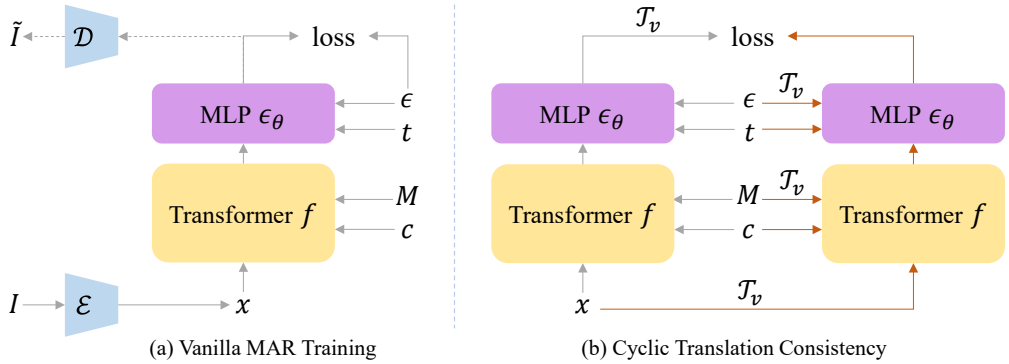

(a) Vanilla MAR Training (b) Cyclic Translation Consistency

Figure 2: **Method illustration.** (a) PAR utilizes a transformer f to predict regions obscured by mask M, then employs these predictions as conditions to drive an MLP ϵ_θ in generating continuous tokens. The VAE encoder $\mathcal{E}$ and decoder $\mathcal{D}$ are frozen. The dashed line indicates the inference phase. c and t denote textual embeddings and time-steps, respectively. (b) Both original and $\mathcal{T}_v$-augmented triples (x, ϵ, M) are processed by the same model, and then aligned through a consistency loss.

As illustrated in Fig. 2 (a), panoramic images I are first compressed into latent representations x using a VAE encoder $\mathcal{E}$. These representations are fed into a transformer model f, which adopts an encoder-decoder architecture. Within the encoder, x is divided into a sequence of visual tokens via patchification. A subset of these tokens is randomly masked by replacing the corresponding regions with a designated [MASK] token. Sine-cosine positional encodings (PEs) are added to the token sequence to preserve spatial information.

Simultaneously, textual prompts are processed by a pre-trained text encoder [26], which encodes them into textual embeddings $c \in \mathbb{R}^d$, where d matches the dimensionality of the visual tokens. The unmasked visual tokens are fused with the textual embeddings c in the encoder, and the resulting contextualized representations are then passed to the decoder, where they are integrated with the masked tokens to facilitate predictive reconstruction.

Unlike the standard AR modeling, the decoder's output is not used as the final result, but as a conditional signal z to drive a lightweight denoising network, which is implemented by a multilayer perceptron (MLP) ϵ_θ. During the training phase, the noise-corrupted x_t is denoised by ϵ_θ under z as follows:

$$\mathcal{L}_{va} = \mathbb{E}_{t,\epsilon}\left[M \circ ||\epsilon_t - \epsilon_\theta(x_t|t, z)||^2\right]. \tag{6}$$

In Eq. 6, $\circ$ is pixel-wise multiplication with binary mask M, where the value corresponding to the masked token is 1. The encoder-decoder f and ϵ_θ are jointly optimized.

Cyclic Translation Consistency. Current foundation models [48, 14] are predominantly trained on perspective images, leading to suboptimal feature representations for ERP-formatted panoramas. We introduce a cyclic translation operator $\mathcal{T}_v$ to address this domain gap and construct semantically equivalent panorama pairs, where v indicates arbitrary translation distance. As shown in Fig. 2 (b), we construct an input pair, (x, ϵ, M) and $(x', \epsilon', M') = (\mathcal{T}_v(x), \mathcal{T}_v(\epsilon), \mathcal{T}_v(M))$. Both inputs share identical PE maps to prevent trivial solutions. The main model processes these pairs to produce outputs y and y', respectively. We enforce equivariance by aligning $\mathcal{T}_v(y)$ with y' only on masked regions through the objective:

$$\mathcal{L}_{consistency} = M' \circ ||\mathcal{T}_v(\epsilon_\theta(x_t|t, x, M)) - \epsilon_\theta(x'_t|t, x', M')||^2, \tag{7}$$

The final learning objective can be written as follows:

$$\mathcal{L} = \mathcal{L}_{va} + \lambda \mathcal{L}_{consistency}, \tag{8}$$

where λ is set as 0.1 in our experiments.

Discussion. The equivariance constraint holds exclusively for ERP panoramas due to their inherent horizontal continuity. For perspective images, applying $\mathcal{T}_v$ artificially creates discontinuous boundaries in the center of the shifted image, which violates two critical premises. 1) *Semantic equivalence*. Unlike panoramas, shifted perspective images lose semantic consistency due to non-periodic scene

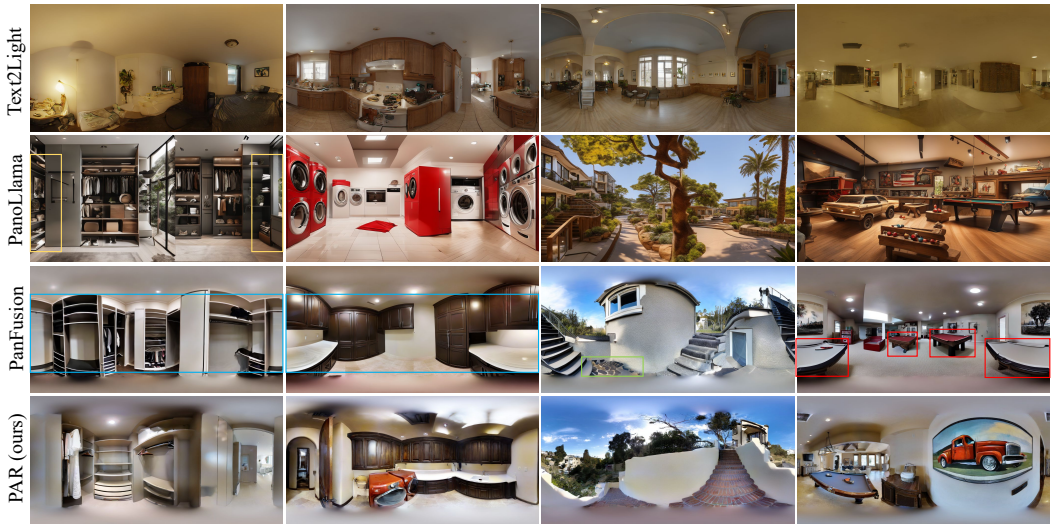

Figure 3: **Visual comparisons with previous methods on text-to-panorama task.** Previous methods neglect the circular consistency characteristics (yellow box), or suffer from repetitive objects (red box), artifact generation (blue box), and inconsistent combinations (green box). The highlighted portions in captions indicate text-image alignment failure cases of baseline methods.

structures. 2) *Model prior*. Generation models inherently enforce feature continuity in image interiors, making it infeasible to produce fragmented content.

Circular Padding. While the AR model incorporates panoramic priors, the VAE's latent space processing may still introduce discontinuities. Standard convolution operations in VAE provide sufficient context for central regions but suffer from information asymmetry at image edges - pixels near boundaries receive unidirectional receptive fields. To address this issue, we propose a dual-space circular padding scheme: pre-padding and post-padding. The former is applied in pixel space for the VAE encoder, while the latter is used in latent space for the VAE decoder. Specifically, we crop a particular portion of the left and right regions and concatenate them to the other side, as formulated in Eq. 9.

$$C_r(x) = \text{concat}(x[..., -rW/2:], x, x[..., :rW/2]), \tag{9}$$

where $x \in \mathbb{R}^{H \times W}$ and $C_r(x) \in \mathbb{R}^{H \times (1+r)W}$, indicate the original and the padded tensor, respectively. r indicates the ratio of padding width to that of the original images or latent variables. After the VAE transformation, the edge positions have sufficient context information. Therefore, the areas that belong to the padding are discarded.

4 Experiment

4.1 Experiment Settings

Implementation Details. We utilize NOVA [14] as the initialization and set the resolution as 512×1024. Our model is trained for 20K iterations with a batch size 32. We employ an AdamW optimizer [35]. The learning rate is 5×10^{-5} with the linear scheduler. In the inference stage, we set the CFG [23] coefficient as 5. In this paper, the masking sequence for training and the sampling sequence for inference are initialized with a uniform distribution unless otherwise stated.

Datasets and Metrics. We mainly use Matterport3D [6] for comparisons. The split of the training and validation set follows PanFusion [74]. We use Janus-Pro-7B [9] to generate the captions.

Table 1: Performance on text-to-panorama task. PO and PE represent panorama outpainting and editing, respectively. **Bold** and underline indicate the first and second best entries.

Modeling	Method	#params	T2P	PO	PE	FAED ↓	FID ↓	CLIP Score ↑	DS ↓
Diffusion	PanFusion [74]	1.9B	✓	-	-	5.12	45.21	31.07	0.71
AR	Text2Light [10]	0.8B	✓	-	-	68.90	70.42	27.90	7.55
	PanoLlama [80]	0.8B	✓	-	-	33.15	103.51	**32.54**	13.99
	PAR (ours)	0.3B	✓	✓	✓	3.39	41.15	30.21	0.58
	PAR (ours)	0.6B	✓	✓	✓	**3.34**	39.31	30.34	**0.57**
	PAR (ours)	1.4B	✓	✓	✓	3.75	**37.37**	30.41	0.58

(a) Mask (b) AOG-Net (c) 2S-ODIS (d) PAR w/o prompt (e) PAR w/ prompt

Figure 4: **Qualitative comparisons of panorama outpainting on the Matterport3D dataset.** PAR-1.4B is used for this task, where PAR w/o prompt means the textual prompt is set as empty.

Several metrics are used in this paper. Fréchet Inception Distance (FID) [21] measures the similarity between the distribution of real and generated images in a feature space derived from a pre-trained inception network. Lower FID scores indicate better realism of synthesized results. CLIP Score (CS) [46] evaluates the alignment between text and image. Furthermore, as FID relies on an Inception network [54] trained on perspective images, we also report the Fréchet Auto-Encoder Distance (FAED) [41] score, which is a variant of FID customized for panorama. To measure the cycle consistency of panoramic images, we adopt Discontinuity Score (DS) [11].

Baselines. Since only a few approaches combine T2P and PO, we compare PAR with specialist methods separately. Specifically, for T2P, we compare with several diffusion-based and AR-based methods, including PanFusion [74], Text2Light [10], and PanoLlama [80]. We take AOG-Net [36] and 2S-ODIS [38] as PO baselines. All experiments are implemented on the Matterport3D dataset.

4.2 Main Results

Text-to-Panorama. Tab. 1 shows the quantitative comparison results. Within the scope of AR-based methods, our PAR significantly outperforms previous approaches regarding generation quality and continuity score. Our method is slightly inferior in the CLIP score metric, probably because CLIP [46] is pre-trained on massive perspective images, and panoramic geometry is not well aligned with perspective images. Moreover, our model performs decently compared with a strong diffusion-based baseline, PanFusion, with only 0.3B parameters. Specifically, PAR-0.3B outperforms PanFusion with 1.73 and 4.06 on FAED and FID, with a discontinuity score of 0.58. Scaling up the parameters helps achieve better results, which is further illustrated in Sec. 4.3.

Fig. 3 provides visual comparisons with the aforementioned baseline methods, including diffusion-based and AR-based models. Our model shows better instruction-following ability, more consistent generation results, and avoids duplicate generation. Specifically, Text2Light cannot obtain satisfactory synthesized results. PanoLlama cannot understand panorama geometry and neglects the characteristic of cycle consistency. PanFusion produces more reasonable results, but sometimes faces artifact problems. For example, the first and second columns of the third row show a room without an exit.

Panorama Outpainting. Tab. 2 compares our method with AOG-Net and 2S-ODIS. We use the model trained with Eq. 8 and inference following Eq. 4, where $\mathcal{S}_k$ indicates the positions within the mask. Our model achieves 32.68 and 12.20 on FID and FID-h, respectively. FID-h is similar to FID, but the difference is that it extracts eight perspective views in the horizontal direction with a 90-degree FoV for each panoramic image, which pays more attention to the generation quality of local regions. Fig. 4 visualizes the synthesized results. Existing methods suffer from local distortion

Table 2: **Panorama outpainting results on the Matterport3D dataset.** For FID-h, we horizontally sample 8 perspective images with FoV=90° for each panorama and then calculate their FID.

Method	T2P	PO	PE	FID ↓	FID-h ↓
AOG-Net [36]	-	✓	-	83.02	37.88
2S-ODIS [38]	-	✓	-	52.59	35.18
PAR w/o prompt	✓	✓	✓	41.63	25.97
PAR w/ prompt	✓	✓	✓	**32.68**	**12.20**

Figure 5: **Scaling parameters and training compute improve fidelity and soundness**. Two cases are shown with 3 model sizes and 3 different training stages. From top to bottom: 0.3B, 0.6B, 1.4B. From left to right: 25%, 50%, 100% of the training process.

(the 3^{rd} column) or counterfactual repetitive structures (the 2^{nd} column). Our method overcomes these problems and still produces reasonable results without textual prompts.

4.3 Ablation Study

Scalability. We train with three different parameter sizes, namely 0.3B, 0.6B, and 1.4B, respectively. In Tab. 1, FID and CS improve with increasing parameters. We also visualize the performance under different training stages, including 25%, 50%, and 100% of the whole training process. As shown in Fig. 5, the improvement of fidelity and soundness is consistent with the scaling of parameters and computation. Larger models learn data distributions better, such as details and panoramic geometry.

Generalization. Fig. 6 visualizes the outpainting results of PAR on OOD data. SUN360 [66] is used for evaluation, which has different data distributions from Matterport3D. PAR shows decent performance across various scenarios. We also compared with several PO baselines trained on the SUN360 dataset. However, Diffusion360 [18] suffers from unrealistic scenes and lacks details. Panodiff [62] also encounters artifact problems (red sky in the 1^{st} row).

PAR can also adapt to different tasks, such as panoramic image editing. As shown in Fig. 7, the model needs to preserve the content inside the mask and regenerate according to new textual prompts. We designed three challenging text prompts, whose content differs from the training datasets, and contains specific conflicts with the original image. For example, fire *vs*. yard in (b), snow *vs*. current season of scene in (c), and ocean *vs*. current place of the scene in (d). Interestingly, our model can generate them well and understands panoramic characteristics. As shown in Fig. 7 (b), the left and right sides of the image can be stitched to form a whole fire.

Translation Equivariance. Tab. 3 demonstrates the effectiveness of consistency loss. Eq. 7 helps the model adapt to panoramic characteristics, thus improving generation quality. Fig. 8 (left) shows the convergence of r. Post-padding significantly improves DS when $r_{post} > 0$ as it helps to smooth stitching seams in the pixel space. However, the model without pre-padding suffers from higher discontinuity, indicating the misalignment between the training and testing phases. With

Table 3: Ablations on cyclic consistency loss.

Method	FID ↓	CLIP Score ↑	DS ↓
w/o $\mathcal{L}_{consistency}$	39.55	30.25	0.57
w/ $\mathcal{L}_{consistency}$	37.37	30.41	0.58

(a) Mask (b) Panodiff (c) Diffusion360 (d) PAR (ours)

Figure 6: **Panorama outpainting on OOD dataset.** The images are from SUN360, which is out of the distribution of our training data. PAR generates realistic panorama images while previous methods have problems like artifacts, or unrealistic results.

(a) Original Image (b) The flames are blazing in the yard (c) A red sports car parked in the snow (d) A house with a view of ocean

Figure 7: **Panoramic image editing**. We design several challenging textual prompts to enforce the model to regenerate the contents outside the red box while maintaining the inside contents. Note that our PAR performs zero-shot task generalization.

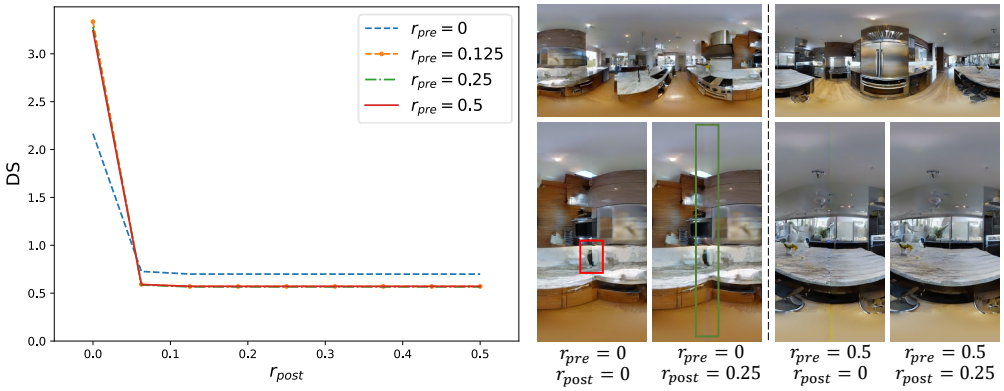

Figure 8: **Left**: The curve of DS about r_{post}. **Right**: Visualizations of different circular padding strategies. Each part consists of three images, where the top one represents the panoramic image generation result, the left and right ones represent the edge stitching results, respectively. The red box indicates the semantic discontinuity, and the green box highlights the seam after post-padding.

the same r_{pre}, DS converges quickly when $r_{post} > 0.125$. A similar phenomenon is observed with r_{post} fixed. Specifically, the curve of $r_{pre} = 0.25$ and $r_{pre} = 0.5$ almost coincide.

Fig. 8 (right) visually explains the difference between the two padding strategies. When $r_{pre} = 0$, semantic inconsistency exists between the left and right edges of the panoramic image. Post-padding cannot repair it even with a large padding ratio, and the green box bounds the smoothed seam. In contrast, the model generates consistent contents when pre-padding is applied.

5 Conclusion

This paper proposes PAR, a MAR-based architecture that unifies text- and image-conditioned panoramic image generation. We delve into the cyclic translation equivariance of ERP panoramas and correspondingly propose a consistency alignment and circular padding strategy. Experiments demonstrate PAR's effectiveness on text-to-panorama and panorama outpainting tasks, whilst showing

promising scalability and generalization capability. We hope our research provides a new solution for the panorama generation community.

Acknowledgement. This work was supported by the National Key Research and Development Program of China (No. 2023YFC3807600).

References

[1] Jinbin Bai, Tian Ye, Wei Chow, Enxin Song, Qing-Guo Chen, Xiangtai Li, Zhen Dong, Lei Zhu, and Shuicheng Yan. Meissonic: Revitalizing masked generative transformers for efficient high-resolution text-to-image synthesis. *arXiv preprint arXiv:2410.08261*, 2024. 3

[2] Omer Bar-Tal, Lior Yariv, Yaron Lipman, and Tali Dekel. Multidiffusion: Fusing diffusion paths for controlled image generation. In *ICML*, 2023. 2

[3] Andreas Blattmann, Tim Dockhorn, Sumith Kulal, Daniel Mendelevitch, Maciej Kilian, Dominik Lorenz, Yam Levi, Zion English, Vikram Voleti, Adam Letts, et al. Stable video diffusion: Scaling latent video diffusion models to large datasets. *arXiv preprint arXiv:2311.15127*, 2023. 3

[4] Tim Brooks, Aleksander Holynski, and Alexei A Efros. Instructpix2pix: Learning to follow image editing instructions. In *CVPR*, 2023. 3

[5] Tom B. Brown, Benjamin Mann, Nick Ryder, Melanie Subbiah, Jared Kaplan, Prafulla Dhariwal, Arvind Neelakantan, Pranav Shyam, Girish Sastry, Amanda Askell, Sandhini Agarwal, Ariel Herbert-Voss, Gretchen Krueger, Tom Henighan, Rewon Child, Aditya Ramesh, Daniel M. Ziegler, Jeffrey Wu, Clemens Winter, Christopher Hesse, Mark Chen, Eric Sigler, Mateusz Litwin, Scott Gray, Benjamin Chess, Jack Clark, Christopher Berner, Sam McCandlish, Alec Radford, Ilya Sutskever, and Dario Amodei. Language models are few-shot learners. In *NeurIPS*, 2020. 3

[6] Angel Chang, Angela Dai, Thomas Funkhouser, Maciej Halber, Matthias Niessner, Manolis Savva, Shuran Song, Andy Zeng, and Yinda Zhang. Matterport3d: Learning from rgb-d data in indoor environments. *arXiv preprint arXiv:1709.06158*, 2017. 2, 6

[7] Huiwen Chang, Han Zhang, Jarred Barber, AJ Maschinot, Jose Lezama, Lu Jiang, Ming-Hsuan Yang, Kevin Murphy, William T Freeman, Michael Rubinstein, et al. Muse: Text-to-image generation via masked generative transformers. *arXiv preprint arXiv:2301.00704*, 2023. 3

[8] Huiwen Chang, Han Zhang, Lu Jiang, Ce Liu, and William T Freeman. Maskgit: Masked generative image transformer. In *CVPR*, 2022. 3

[9] Xiaokang Chen, Zhiyu Wu, Xingchao Liu, Zizheng Pan, Wen Liu, Zhenda Xie, Xingkai Yu, and Chong Ruan. Janus-pro: Unified multimodal understanding and generation with data and model scaling. *arXiv preprint arXiv:2501.17811*, 2025. 6

[10] Zhaoxi Chen, Guangcong Wang, and Ziwei Liu. Text2light: Zero-shot text-driven hdr panorama generation. *ACM Transactions on Graphics*, 2022. 3, 7

[11] Anders Christensen, Nooshin Mojab, Khushman Patel, Karan Ahuja, Zeynep Akata, Ole Winther, Mar Gonzalez-Franco, and Andrea Colaco. Geometry fidelity for spherical images. In *ECCV*, 2024. 7

[12] Thiago LT da Silveira, Paulo GL Pinto, Jeffri Murrugarra-Llerena, and Cláudio R Jung. 3d scene geometry estimation from 360 imagery: A survey. *ACM Computing Surveys*, 2022. 2

[13] Mohammad Reza Karimi Dastjerdi, Yannick Hold-Geoffroy, Jonathan Eisenmann, Siavash Khodadadeh, and Jean-François Lalonde. Guided co-modulated gan for 360 field of view extrapolation. In *3DV*, 2022. 2

[14] Haoge Deng, Ting Pan, Haiwen Diao, Zhengxiong Luo, Yufeng Cui, Huchuan Lu, Shiguang Shan, Yonggang Qi, and Xinlong Wang. Autoregressive video generation without vector quantization. *arXiv preprint arXiv:2412.14169*, 2024. 3, 4, 5, 6

[15] Ming Ding, Zhuoyi Yang, Wenyi Hong, Wendi Zheng, Chang Zhou, Da Yin, Junyang Lin, Xu Zou, Zhou Shao, Hongxia Yang, et al. Cogview: Mastering text-to-image generation via transformers. In *NeurIPS*, 2021. 3

[16] Ming Ding, Wendi Zheng, Wenyi Hong, and Jie Tang. Cogview2: Faster and better text-to-image generation via hierarchical transformers. In *NeurIPS*, 2022. 3

[17] Patrick Esser, Sumith Kulal, Andreas Blattmann, Rahim Entezari, Jonas Müller, Harry Saini, Yam Levi, Dominik Lorenz, Axel Sauer, Frederic Boesel, et al. Scaling rectified flow transformers for high-resolution image synthesis. In *ICML*, 2024. 3

[18] Mengyang Feng, Jinlin Liu, Miaomiao Cui, and Xuansong Xie. Diffusion360: Seamless 360 degree panoramic image generation based on diffusion models. *arXiv preprint arXiv:2311.13141*, 2023. 2, 8, 25

[19] Penglei Gao, Kai Yao, Tiandi Ye, Steven Wang, Yuan Yao, and Xiaofeng Wang. Opa-ma: Text guided mamba for 360-degree image out-painting. *arXiv preprint arXiv:2407.10923*, 2024. 2, 3

[20] William Harvey, Saeid Naderiparizi, Vaden Masrani, Christian Weilbach, and Frank Wood. Flexible diffusion modeling of long videos. In *NeurIPS*, 2022. 3

[21] Martin Heusel, Hubert Ramsauer, Thomas Unterthiner, Bernhard Nessler, and Sepp Hochreiter. Gans trained by a two time-scale update rule converge to a local nash equilibrium. In *NeurIPS*, 2017. 7

[22] Jonathan Ho, Chitwan Saharia, William Chan, David J Fleet, Mohammad Norouzi, and Tim Salimans. Cascaded diffusion models for high fidelity image generation. *The Journal of Machine Learning Research*, 2022. 3

[23] Jonathan Ho and Tim Salimans. Classifier-free diffusion guidance. In *NeurIPS Workshops*, 2021. 3, 6

[24] Wenyi Hong, Ming Ding, Wendi Zheng, Xinghan Liu, and Jie Tang. Cogvideo: Large-scale pretraining for text-to-video generation via transformers. *arXiv preprint arXiv:2205.15868*, 2022. 3

[25] Kuan-Chih Huang, Xiangtai Li, Lu Qi, Shuicheng Yan, and Ming-Hsuan Yang. Reason3d: Searching and reasoning 3d segmentation via large language model. In *3DV*, 2025. 2

[26] Mojan Javaheripi, Sébastien Bubeck, Marah Abdin, Jyoti Aneja, Sebastien Bubeck, Caio César Teodoro Mendes, Weizhu Chen, Allie Del Giorno, Ronen Eldan, Sivakanth Gopi, et al. Phi-2: The surprising power of small language models. *Microsoft Research Blog*, 2023. 5

[27] Nikolai Kalischek, Michael Oechsle, Fabian Manhardt, Philipp Henzler, Konrad Schindler, and Federico Tombari. Cubediff: Repurposing diffusion-based image models for panorama generation. *arXiv preprint arXiv:2501.17162*, 2025. 2, 3

[28] Dan Kondratyuk, Lijun Yu, Xiuye Gu, José Lezama, Jonathan Huang, Rachel Hornung, Hartwig Adam, Hassan Akbari, Yair Alon, Vighnesh Birodkar, et al. Videopoet: A large language model for zero-shot video generation. *arXiv preprint arXiv:2312.14125*, 2023. 3

[29] Jialu Li and Mohit Bansal. Panogen: Text-conditioned panoramic environment generation for vision-and-language navigation. In *NeurIPS*, 2023. 2, 3

[30] Tianhong Li, Yonglong Tian, He Li, Mingyang Deng, and Kaiming He. Autoregressive image generation without vector quantization. In *NeurIPS*, 2024. 2, 3

[31] Yaron Lipman, Ricky TQ Chen, Heli Ben-Hamu, Maximilian Nickel, and Matt Le. Flow matching for generative modeling. In *ICLR*, 2023. 3

[32] Xingchao Liu, Chengyue Gong, and Qiang Liu. Flow straight and fast: Learning to generate and transfer data with rectified flow. In *ICLR*, 2023. 3

[33] Xingchao Liu, Xiwen Zhang, Jianzhu Ma, Jian Peng, et al. Instaflow: One step is enough for high-quality diffusion-based text-to-image generation. In *ICLR*, 2024. 3

[34] Yuheng Liu, Xinke Li, Xueting Li, Lu Qi, Chongshou Li, and Ming-Hsuan Yang. Pyramid diffusion for fine 3d large scene generation. In *ECCV*, 2024. 2

[35] Ilya Loshchilov, Frank Hutter, et al. Fixing weight decay regularization in adam. *arXiv preprint arXiv:1711.05101*, 2017. 6

[36] Zhuqiang Lu, Kun Hu, Chaoyue Wang, Lei Bai, and Zhiyong Wang. Autoregressive omni-aware outpainting for open-vocabulary 360-degree image generation. In *AAAI*, 2024. 2, 3, 7, 8

[37] Andreas Lugmayr, Martin Danelljan, Andres Romero, Fisher Yu, Radu Timofte, and Luc Van Gool. Repaint: Inpainting using denoising diffusion probabilistic models. In *CVPR*, 2022. 3

[38] Atsuya Nakata and Takao Yamanaka. 2s-odis: Two-stage omni-directional image synthesis by geometric distortion correction. In *ECCV*, 2024. 7, 8

[39] Charlie Nash, Joao Carreira, Jacob Walker, Iain Barr, Andrew Jaegle, Mateusz Malinowski, and Peter Battaglia. Transframer: Arbitrary frame prediction with generative models. *arXiv preprint arXiv:2203.09494*, 2022. 3

[40] Jinhong Ni, Chang-Bin Zhang, Qiang Zhang, and Jing Zhang. What makes for text to 360-degree panorama generation with stable diffusion? *ICCV*, 2025. 23

[41] Changgyoon Oh, Wonjune Cho, Yujeong Chae, Daehee Park, Lin Wang, and Kuk-Jin Yoon. Bips: Bi-modal indoor panorama synthesis via residual depth-aided adversarial learning. In *ECCV*, 2022. 7

[42] William Peebles and Saining Xie. Scalable diffusion models with transformers. In *ICCV*, 2023. 3

[43] Dustin Podell, Zion English, Kyle Lacey, Andreas Blattmann, Tim Dockhorn, Jonas Müller, Joe Penna, and Robin Rombach. Sdxl: Improving latent diffusion models for high-resolution image synthesis. In *ICLR*, 2024. 2, 3

[44] Lu Qi, Li Jiang, Shu Liu, Xiaoyong Shen, and Jiaya Jia. Amodal instance segmentation with kins dataset. In *CVPR*, 2019. 2

[45] Yu Qiu, Xin Lin, Jingbo Wang, Xiangtai Li, Lu Qi, and Ming-Hsuan Yang. Umc: Unified resilient controller for legged robots with joint malfunctions. In *arXiv*, 2025. 2

[46] Alec Radford, Jong Wook Kim, Chris Hallacy, Aditya Ramesh, Gabriel Goh, Sandhini Agarwal, Girish Sastry, Amanda Askell, Pamela Mishkin, Jack Clark, et al. Learning transferable visual models from natural language supervision. In *ICML*, 2021. 7

[47] Aditya Ramesh, Mikhail Pavlov, Gabriel Goh, Scott Gray, Chelsea Voss, Alec Radford, Mark Chen, and Ilya Sutskever. Zero-shot text-to-image generation. In *ICML*, 2021. 3

[48] Robin Rombach, Andreas Blattmann, Dominik Lorenz, Patrick Esser, and Björn Ommer. High-resolution image synthesis with latent diffusion models. In *CVPR*, 2022. 2, 3, 5

[49] Chitwan Saharia, William Chan, Huiwen Chang, Chris Lee, Jonathan Ho, Tim Salimans, David Fleet, and Mohammad Norouzi. Palette: Image-to-image diffusion models. In *SIGGRAPH*, 2022. 3

[50] Chitwan Saharia, Jonathan Ho, William Chan, Tim Salimans, David J Fleet, and Mohammad Norouzi. Image super-resolution via iterative refinement. *TPAMI*, 2022. 3

[51] Jiaming Song, Chenlin Meng, and Stefano Ermon. Denoising diffusion implicit models. In *ICLR*, 2021. 3

[52] Yang Song, Jascha Sohl-Dickstein, Diederik P Kingma, Abhishek Kumar, Stefano Ermon, and Ben Poole. Score-based generative modeling through stochastic differential equations. In *ICLR*, 2021. 3

[53] Peize Sun, Yi Jiang, Shoufa Chen, Shilong Zhang, Bingyue Peng, Ping Luo, and Zehuan Yuan. Autoregressive model beats diffusion: Llama for scalable image generation. *arXiv preprint arXiv:2406.06525*, 2024. 3

[54] Christian Szegedy, Vincent Vanhoucke, Sergey Ioffe, Jon Shlens, and Zbigniew Wojna. Rethinking the inception architecture for computer vision. In *CVPR*, 2016. 7

[55] Jing Tan, Shuai Yang, Tong Wu, Jingwen He, Yuwei Guo, Ziwei Liu, and Dahua Lin. Imagine360: Immersive 360 video generation from perspective anchor. *arXiv preprint arXiv:2412.03552*, 2024. 2, 3

[56] Shitao Tang, Jiacheng Chen, Dilin Wang, Chengzhou Tang, Fuyang Zhang, Yuchen Fan, Vikas Chandra, Yasutaka Furukawa, and Rakesh Ranjan. Mvdiffusion++: A dense high-resolution multi-view diffusion model for single or sparse-view 3d object reconstruction. In *ECCV*, 2024. 2

[57] Shitao Tang, Fuyang Zhang, Jiacheng Chen, Peng Wang, and Yasutaka Furukawa. Mvdiffusion: Enabling holistic multi-view image generation with correspondence-aware diffusion. In *NeurIPS*, 2023. 2, 3

[58] Hugo Touvron, Louis Martin, Kevin Stone, Peter Albert, Amjad Almahairi, Yasmine Babaei, Nikolay Bashlykov, Soumya Batra, Prajjwal Bhargava, Shruti Bhosale, et al. Llama 2: Open foundation and fine-tuned chat models. *arXiv: 2307.09288*, 2023. 3

[59] Ruben Villegas, Mohammad Babaeizadeh, Pieter-Jan Kindermans, Hernan Moraldo, Han Zhang, Mohammad Taghi Saffar, Santiago Castro, Julius Kunze, and Dumitru Erhan. Phenaki: Variable length video generation from open domain textual descriptions. In *ICLR*, 2022. 3

[60] Zhaoliang Wan, Yonggen Ling, Senlin Yi, Lu Qi, Wangwei Lee, Minglei Lu, Sicheng Yang, Xiao Teng, Peng Lu, Xu Yang, et al. Vint-6d: A large-scale object-in-hand dataset from vision, touch and proprioception. In *ICML*, 2024. 2

[61] Hai Wang, Xiaoyu Xiang, Yuchen Fan, and Jing-Hao Xue. Customizing 360-degree panoramas through text-to-image diffusion models. In *WACV*, 2024. 23

[62] Jionghao Wang, Ziyu Chen, Jun Ling, Rong Xie, and Li Song. 360-degree panorama generation from few unregistered nfov images. *arXiv preprint arXiv:2308.14686*, 2023. 2, 8, 24

[63] Yuqing Wang, Tianwei Xiong, Daquan Zhou, Zhijie Lin, Yang Zhao, Bingyi Kang, Jiashi Feng, and Xihui Liu. Loong: Generating minute-level long videos with autoregressive language models. *arXiv preprint arXiv:2410.02757*, 2024. 3

[64] Tao Wu, Xuewei Li, Zhongang Qi, Di Hu, Xintao Wang, Ying Shan, and Xi Li. Spherediffusion: Spherical geometry-aware distortion resilient diffusion model. In *AAAI*, 2024. 2

[65] Tianhao Wu, Chuanxia Zheng, and Tat-Jen Cham. Panodiffusion: 360-degree panorama outpainting via diffusion. *arXiv preprint arXiv:2307.03177*, 2023. 2

[66] Jianxiong Xiao, Krista A Ehinger, Aude Oliva, and Antonio Torralba. Recognizing scene viewpoint using panoramic place representation. In *CVPR*, 2012. 8

[67] Wilson Yan, Yunzhi Zhang, Pieter Abbeel, and Aravind Srinivas. Videogpt: Video generation using vq-vae and transformers. *arXiv preprint arXiv:2104.10157*, 2021. 3

[68] Liu Yang, Huiyu Duan, Yucheng Zhu, Xiaohong Liu, Lu Liu, Zitong Xu, Guangji Ma, Xiongkuo Min, Guangtao Zhai, and Patrick Le Callet. Omni ^{2}: Unifying omnidirectional image generation and editing in an omni model. *arXiv preprint arXiv:2504.11379*, 2025. 2, 3

[69] Ruihan Yang, Prakhar Srivastava, and Stephan Mandt. Diffusion probabilistic modeling for video generation. *Entropy*, 2023. 3

[70] Weicai Ye, Chenhao Ji, Zheng Chen, Junyao Gao, Xiaoshui Huang, Song-Hai Zhang, Wanli Ouyang, Tong He, Cairong Zhao, and Guofeng Zhang. Diffpano: Scalable and consistent text to panorama generation with spherical epipolar-aware diffusion. *arXiv preprint arXiv:2410.24203*, 2024. 2, 23

[71] Fanghua Yu, Jinjin Gu, Zheyuan Li, Jinfan Hu, Xiangtao Kong, Xintao Wang, Jingwen He, Yu Qiao, and Chao Dong. Scaling up to excellence: Practicing model scaling for photo-realistic image restoration in the wild. In *CVPR*, 2024. 3

[72] Jiahui Yu, Yuanzhong Xu, Jing Yu Koh, Thang Luong, Gunjan Baid, Zirui Wang, Vijay Vasudevan, Alexander Ku, Yinfei Yang, Burcu Karagol Ayan, et al. Scaling autoregressive models for content-rich text-to-image generation. *arXiv preprint arXiv:2206.10789*, 2022. 3

[73] Lijun Yu, Yong Cheng, Kihyuk Sohn, José Lezama, Han Zhang, Huiwen Chang, Alexander G Hauptmann, Ming-Hsuan Yang, Yuan Hao, Irfan Essa, et al. Magvit: Masked generative video transformer. In *CVPR*, 2023. 3

[74] Cheng Zhang, Qianyi Wu, Camilo Cruz Gambardella, Xiaoshui Huang, Dinh Phung, Wanli Ouyang, and Jianfei Cai. Taming stable diffusion for text to 360 panorama image generation. In *CVPR*, 2024. 2, 3, 6, 7

[75] Lvmin Zhang, Anyi Rao, and Maneesh Agrawala. Adding conditional control to text-to-image diffusion models. In *ICCV*, 2023. 3

[76] Xiaoyu Zhang, Teng Zhou, Xinlong Zhang, Jia Wei, and Yongchuan Tang. Multi-scale diffusion: Enhancing spatial layout in high-resolution panoramic image generation. *arXiv preprint arXiv:2410.18830*, 2024. 2

[77] Dian Zheng, Cheng Zhang, Xiao-Ming Wu, Cao Li, Chengfei Lv, Jian-Fang Hu, and Wei-Shi Zheng. Panorama generation from nfov image done right. *arXiv preprint arXiv:2503.18420*, 2025. 2

[78] Jia Zheng, Junfei Zhang, Jing Li, Rui Tang, Shenghua Gao, and Zihan Zhou. Structured3d: A large photo-realistic dataset for structured 3d modeling. In *ECCV*, 2020. 23

[79] Junwei Zhou, Xueting Li, Lu Qi, and Ming-Hsuan Yang. Layout-your-3d: Controllable and precise 3d generation with 2d blueprint. In *ICLR*, 2025. 2

[80] Teng Zhou, Xiaoyu Zhang, and Yongchuan Tang. Panollama: Generating endless and coherent panoramas with next-token-prediction llms. *arXiv preprint arXiv:2411.15867*, 2024. 3, 7, 25

NeurIPS Paper Checklist

1. **Claims**

   Question: Do the main claims made in the abstract and introduction accurately reflect the paper's contributions and scope?

   Answer: [Yes]

   Justification: We include the main claims in the abstract and introduction.

   Guidelines:

   - The answer NA means that the abstract and introduction do not include the claims made in the paper.
   - The abstract and/or introduction should clearly state the claims made, including the contributions made in the paper and important assumptions and limitations. A No or NA answer to this question will not be perceived well by the reviewers.
   - The claims made should match theoretical and experimental results, and reflect how much the results can be expected to generalize to other settings.
   - It is fine to include aspirational goals as motivation as long as it is clear that these goals are not attained by the paper.

2. **Limitations**

   Question: Does the paper discuss the limitations of the work performed by the authors?

   Answer: [Yes]

   Justification: We discuss the limitations in the appendix.

   Guidelines:

   - The answer NA means that the paper has no limitation while the answer No means that the paper has limitations, but those are not discussed in the paper.
   - The authors are encouraged to create a separate "Limitations" section in their paper.
   - The paper should point out any strong assumptions and how robust the results are to violations of these assumptions (e.g., independence assumptions, noiseless settings, model well-specification, asymptotic approximations only holding locally). The authors should reflect on how these assumptions might be violated in practice and what the implications would be.
   - The authors should reflect on the scope of the claims made, e.g., if the approach was only tested on a few datasets or with a few runs. In general, empirical results often depend on implicit assumptions, which should be articulated.
   - The authors should reflect on the factors that influence the performance of the approach. For example, a facial recognition algorithm may perform poorly when image resolution is low or images are taken in low lighting. Or a speech-to-text system might not be used reliably to provide closed captions for online lectures because it fails to handle technical jargon.
   - The authors should discuss the computational efficiency of the proposed algorithms and how they scale with dataset size.
   - If applicable, the authors should discuss possible limitations of their approach to address problems of privacy and fairness.
   - While the authors might fear that complete honesty about limitations might be used by reviewers as grounds for rejection, a worse outcome might be that reviewers discover limitations that aren't acknowledged in the paper. The authors should use their best judgment and recognize that individual actions in favor of transparency play an important role in developing norms that preserve the integrity of the community. Reviewers will be specifically instructed to not penalize honesty concerning limitations.

3. **Theory assumptions and proofs**

   Question: For each theoretical result, does the paper provide the full set of assumptions and a complete (and correct) proof?

   Answer: [Yes]

Justification: The proof is in the appendix.

Guidelines:

- The answer NA means that the paper does not include theoretical results.
- All the theorems, formulas, and proofs in the paper should be numbered and cross-referenced.
- All assumptions should be clearly stated or referenced in the statement of any theorems.
- The proofs can either appear in the main paper or the supplemental material, but if they appear in the supplemental material, the authors are encouraged to provide a short proof sketch to provide intuition.
- Inversely, any informal proof provided in the core of the paper should be complemented by formal proofs provided in appendix or supplemental material.
- Theorems and Lemmas that the proof relies upon should be properly referenced.

4. **Experimental result reproducibility**

   Question: Does the paper fully disclose all the information needed to reproduce the main experimental results of the paper to the extent that it affects the main claims and/or conclusions of the paper (regardless of whether the code and data are provided or not)?

   Answer: [Yes]

   Justification: We provide details on the implementation in Sec. 4 and appendix.

   Guidelines:

   - The answer NA means that the paper does not include experiments.
   - If the paper includes experiments, a No answer to this question will not be perceived well by the reviewers: Making the paper reproducible is important, regardless of whether the code and data are provided or not.
   - If the contribution is a dataset and/or model, the authors should describe the steps taken to make their results reproducible or verifiable.
   - Depending on the contribution, reproducibility can be accomplished in various ways. For example, if the contribution is a novel architecture, describing the architecture fully might suffice, or if the contribution is a specific model and empirical evaluation, it may be necessary to either make it possible for others to replicate the model with the same dataset, or provide access to the model. In general. releasing code and data is often one good way to accomplish this, but reproducibility can also be provided via detailed instructions for how to replicate the results, access to a hosted model (e.g., in the case of a large language model), releasing of a model checkpoint, or other means that are appropriate to the research performed.
   - While NeurIPS does not require releasing code, the conference does require all submissions to provide some reasonable avenue for reproducibility, which may depend on the nature of the contribution. For example
     (a) If the contribution is primarily a new algorithm, the paper should make it clear how to reproduce that algorithm.
     (b) If the contribution is primarily a new model architecture, the paper should describe the architecture clearly and fully.
     (c) If the contribution is a new model (e.g., a large language model), then there should either be a way to access this model for reproducing the results or a way to reproduce the model (e.g., with an open-source dataset or instructions for how to construct the dataset).
     (d) We recognize that reproducibility may be tricky in some cases, in which case authors are welcome to describe the particular way they provide for reproducibility. In the case of closed-source models, it may be that access to the model is limited in some way (e.g., to registered users), but it should be possible for other researchers to have some path to reproducing or verifying the results.

5. **Open access to data and code**

   Question: Does the paper provide open access to the data and code, with sufficient instructions to faithfully reproduce the main experimental results, as described in supplemental material?

Answer: [Yes]

Justification: The code is released.

Guidelines:

- The answer NA means that paper does not include experiments requiring code.
- Please see the NeurIPS code and data submission guidelines (https://nips.cc/public/guides/CodeSubmissionPolicy) for more details.
- While we encourage the release of code and data, we understand that this might not be possible, so "No" is an acceptable answer. Papers cannot be rejected simply for not including code, unless this is central to the contribution (e.g., for a new open-source benchmark).
- The instructions should contain the exact command and environment needed to run to reproduce the results. See the NeurIPS code and data submission guidelines (https://nips.cc/public/guides/CodeSubmissionPolicy) for more details.
- The authors should provide instructions on data access and preparation, including how to access the raw data, preprocessed data, intermediate data, and generated data, etc.
- The authors should provide scripts to reproduce all experimental results for the new proposed method and baselines. If only a subset of experiments are reproducible, they should state which ones are omitted from the script and why.
- At submission time, to preserve anonymity, the authors should release anonymized versions (if applicable).
- Providing as much information as possible in supplemental material (appended to the paper) is recommended, but including URLs to data and code is permitted.

6. **Experimental setting/details**

   Question: Does the paper specify all the training and test details (e.g., data splits, hyperparameters, how they were chosen, type of optimizer, etc.) necessary to understand the results?

   Answer: [Yes]

   Justification: Experimental setting and details are in Sec. 4.

   Guidelines:

   - The answer NA means that the paper does not include experiments.
   - The experimental setting should be presented in the core of the paper to a level of detail that is necessary to appreciate the results and make sense of them.
   - The full details can be provided either with the code, in appendix, or as supplemental material.

7. **Experiment statistical significance**

   Question: Does the paper report error bars suitably and correctly defined or other appropriate information about the statistical significance of the experiments?

   Answer: [No]

   Justification: We did not conduct experiments with error bars.

   Guidelines:

   - The answer NA means that the paper does not include experiments.
   - The authors should answer "Yes" if the results are accompanied by error bars, confidence intervals, or statistical significance tests, at least for the experiments that support the main claims of the paper.
   - The factors of variability that the error bars are capturing should be clearly stated (for example, train/test split, initialization, random drawing of some parameter, or overall run with given experimental conditions).
   - The method for calculating the error bars should be explained (closed form formula, call to a library function, bootstrap, etc.)
   - The assumptions made should be given (e.g., Normally distributed errors).
   - It should be clear whether the error bar is the standard deviation or the standard error of the mean.

- It is OK to report 1-sigma error bars, but one should state it. The authors should preferably report a 2-sigma error bar than state that they have a 96% CI, if the hypothesis of Normality of errors is not verified.
- For asymmetric distributions, the authors should be careful not to show in tables or figures symmetric error bars that would yield results that are out of range (e.g. negative error rates).
- If error bars are reported in tables or plots, The authors should explain in the text how they were calculated and reference the corresponding figures or tables in the text.

8. **Experiments compute resources**

   Question: For each experiment, does the paper provide sufficient information on the computer resources (type of compute workers, memory, time of execution) needed to reproduce the experiments?

   Answer: [Yes]

   Justification: We provide details of computation cost in the appendix.

   Guidelines:

   - The answer NA means that the paper does not include experiments.
   - The paper should indicate the type of compute workers CPU or GPU, internal cluster, or cloud provider, including relevant memory and storage.
   - The paper should provide the amount of compute required for each of the individual experimental runs as well as estimate the total compute.
   - The paper should disclose whether the full research project required more compute than the experiments reported in the paper (e.g., preliminary or failed experiments that didn't make it into the paper).

9. **Code of ethics**

   Question: Does the research conducted in the paper conform, in every respect, with the NeurIPS Code of Ethics https://neurips.cc/public/EthicsGuidelines?

   Answer: [Yes]

   Justification: We conducted in the paper conform, in every respect, with the NeurIPS Code of Ethics .

   Guidelines:

   - The answer NA means that the authors have not reviewed the NeurIPS Code of Ethics.
   - If the authors answer No, they should explain the special circumstances that require a deviation from the Code of Ethics.
   - The authors should make sure to preserve anonymity (e.g., if there is a special consideration due to laws or regulations in their jurisdiction).

10. **Broader impacts**

    Question: Does the paper discuss both potential positive societal impacts and negative societal impacts of the work performed?

    Answer: [Yes]

    Justification: We discuss the broader impact in the appendix.

    Guidelines:

    - The answer NA means that there is no societal impact of the work performed.
    - If the authors answer NA or No, they should explain why their work has no societal impact or why the paper does not address societal impact.
    - Examples of negative societal impacts include potential malicious or unintended uses (e.g., disinformation, generating fake profiles, surveillance), fairness considerations (e.g., deployment of technologies that could make decisions that unfairly impact specific groups), privacy considerations, and security considerations.

- The conference expects that many papers will be foundational research and not tied to particular applications, let alone deployments. However, if there is a direct path to any negative applications, the authors should point it out. For example, it is legitimate to point out that an improvement in the quality of generative models could be used to generate deepfakes for disinformation. On the other hand, it is not needed to point out that a generic algorithm for optimizing neural networks could enable people to train models that generate Deepfakes faster.
- The authors should consider possible harms that could arise when the technology is being used as intended and functioning correctly, harms that could arise when the technology is being used as intended but gives incorrect results, and harms following from (intentional or unintentional) misuse of the technology.
- If there are negative societal impacts, the authors could also discuss possible mitigation strategies (e.g., gated release of models, providing defenses in addition to attacks, mechanisms for monitoring misuse, mechanisms to monitor how a system learns from feedback over time, improving the efficiency and accessibility of ML).

11. **Safeguards**

    Question: Does the paper describe safeguards that have been put in place for responsible release of data or models that have a high risk for misuse (e.g., pretrained language models, image generators, or scraped datasets)?

    Answer: [Yes]

    Justification: We discuss the broader impact in the appendix.

    Guidelines:

    - The answer NA means that the paper poses no such risks.
    - Released models that have a high risk for misuse or dual-use should be released with necessary safeguards to allow for controlled use of the model, for example by requiring that users adhere to usage guidelines or restrictions to access the model or implementing safety filters.
    - Datasets that have been scraped from the Internet could pose safety risks. The authors should describe how they avoided releasing unsafe images.
    - We recognize that providing effective safeguards is challenging, and many papers do not require this, but we encourage authors to take this into account and make a best faith effort.

12. **Licenses for existing assets**

    Question: Are the creators or original owners of assets (e.g., code, data, models), used in the paper, properly credited and are the license and terms of use explicitly mentioned and properly respected?

    Answer: [Yes]

    Justification: We use existing assets with properly credited.

    Guidelines:

    - The answer NA means that the paper does not use existing assets.
    - The authors should cite the original paper that produced the code package or dataset.
    - The authors should state which version of the asset is used and, if possible, include a URL.
    - The name of the license (e.g., CC-BY 4.0) should be included for each asset.
    - For scraped data from a particular source (e.g., website), the copyright and terms of service of that source should be provided.
    - If assets are released, the license, copyright information, and terms of use in the package should be provided. For popular datasets, `paperswithcode.com/datasets` has curated licenses for some datasets. Their licensing guide can help determine the license of a dataset.
    - For existing datasets that are re-packaged, both the original license and the license of the derived asset (if it has changed) should be provided.

- If this information is not available online, the authors are encouraged to reach out to the asset's creators.

13. **New assets**

    Question: Are new assets introduced in the paper well documented and is the documentation provided alongside the assets?

    Answer: [NA]

    Justification: The paper does not release new assets.

    Guidelines:

    - The answer NA means that the paper does not release new assets.
    - Researchers should communicate the details of the dataset/code/model as part of their submissions via structured templates. This includes details about training, license, limitations, etc.
    - The paper should discuss whether and how consent was obtained from people whose asset is used.
    - At submission time, remember to anonymize your assets (if applicable). You can either create an anonymized URL or include an anonymized zip file.

14. **Crowdsourcing and research with human subjects**

    Question: For crowdsourcing experiments and research with human subjects, does the paper include the full text of instructions given to participants and screenshots, if applicable, as well as details about compensation (if any)?

    Answer: [NA]

    Justification: The paper does not involve crowdsourcing nor research with human subjects.

    Guidelines:

    - The answer NA means that the paper does not involve crowdsourcing nor research with human subjects.
    - Including this information in the supplemental material is fine, but if the main contribution of the paper involves human subjects, then as much detail as possible should be included in the main paper.
    - According to the NeurIPS Code of Ethics, workers involved in data collection, curation, or other labor should be paid at least the minimum wage in the country of the data collector.

15. **Institutional review board (IRB) approvals or equivalent for research with human subjects**

    Question: Does the paper describe potential risks incurred by study participants, whether such risks were disclosed to the subjects, and whether Institutional Review Board (IRB) approvals (or an equivalent approval/review based on the requirements of your country or institution) were obtained?

    Answer: [NA]

    Justification: The paper does not involve crowdsourcing nor research with human subjects.

    Guidelines:

    - The answer NA means that the paper does not involve crowdsourcing nor research with human subjects.
    - Depending on the country in which research is conducted, IRB approval (or equivalent) may be required for any human subjects research. If you obtained IRB approval, you should clearly state this in the paper.
    - We recognize that the procedures for this may vary significantly between institutions and locations, and we expect authors to adhere to the NeurIPS Code of Ethics and the guidelines for their institution.
    - For initial submissions, do not include any information that would break anonymity (if applicable), such as the institution conducting the review.

16. **Declaration of LLM usage**

Question: Does the paper describe the usage of LLMs if it is an important, original, or non-standard component of the core methods in this research? Note that if the LLM is used only for writing, editing, or formatting purposes and does not impact the core methodology, scientific rigorousness, or originality of the research, declaration is not required.

Answer: [NA]

Justification: The core method development in this research does not involve LLMs as any important, original, or non-standard components.

Guidelines:

- The answer NA means that the core method development in this research does not involve LLMs as any important, original, or non-standard components.
- Please refer to our LLM policy (https://neurips.cc/Conferences/2025/LLM) for what should or should not be described.

Overview. In this appendix, we present more results and details:

- **A.** Proof of non-*i.i.d.* of ERP transformation.
- **B.** More details on method.
- **C.** More empirical studies and visual results.
- **D.** Discussion of the broader impacts, safeguards and limitations.

A Proof of Non-*i.i.d.* of ERP Transformation

A.1 Problem Setting

Let the unit sphere

$$\mathbb{S}^2 = \{(x, y, z) \in \mathbb{R}^3 \,:\, x^2 + y^2 + z^2 = 1\}$$

be parameterised by spherical angles $(\phi, \theta) \in (-\pi, \pi] \times [0, \pi]$. The equirectangular projection of spatial resolution $(H, W) \in \mathbb{N}^2$ is the mapping

$$T : [0, W) \times [0, H) \longrightarrow (-\pi, \pi] \times [0, \pi], \qquad (u, v) \mapsto \Big(\phi(u), \theta(v)\Big)$$

with

$$\phi(u) = \frac{2\pi u}{W} - \pi, \qquad \theta(v) = \frac{\pi v}{H}.$$

Conversely, $u = \dfrac{\phi + \pi}{2\pi} W,\ v = \dfrac{\theta}{\pi} H.$

A.2 Gaussian noise field on the sphere

Let $\{\, \varepsilon(\phi, \theta) \,\}_{(\phi,\theta)\in(-\pi,\pi]\times[0,\pi]}$ be a Gaussian noise field on the sphere, i.e.

$$\mathbb{E}[\varepsilon(\phi, \theta)] = 0, \qquad \mathrm{Cov}\big(\varepsilon(\phi, \theta), \varepsilon(\phi', \theta')\big) = \sigma^2\, \delta(\phi - \phi')\, \delta(\theta - \theta'), \tag{10}$$

where δ is the Dirac distribution and $\sigma^2 > 0$ is a constant variance density (per steradian).

A.3 Pixel value definition in ERP

Each ERP pixel $(u, v) \in \{0, \dots, W-1\} \times \{0, \dots, H-1\}$ covers a spherical patch

$$P_{uv} \;=\; \Big[\phi(u - \tfrac{1}{2}), \phi(u + \tfrac{1}{2})\Big) \times \Big[\theta(v - \tfrac{1}{2}), \theta(v + \tfrac{1}{2})\Big).$$

Its area is

$$A_{uv} = \int_{P_{uv}} \sin\theta \, d\phi \, d\theta \;=\; \frac{2\pi}{W} \left[\cos\theta(v - \tfrac{1}{2}) - \cos\theta(v + \tfrac{1}{2})\right] \;=\; \frac{2\pi^2}{WH} \sin\theta_v, \tag{11}$$

with the mid-latitude $\theta_v := \theta(v) = \pi v / H$.

The *noise value stored in the pixel* is the area–average

$$\eta_{uv} := \frac{1}{A_{uv}} \int_{P_{uv}} \varepsilon(\phi, \theta)\, dA, \quad dA = \sin\theta \, d\phi \, d\theta. \tag{12}$$

Because the integral in Eq. 12 is a *linear* functional of the Gaussian field ε, each η_{uv} is still Gaussian.

A.4 Independence

For two different pixels $(u, v) \neq (u', v')$ the patches $P_{uv}, P_{u'v'}$ are disjoint. Since Eq. 10 states that $\varepsilon(\phi, \theta)$ is white, integrals over disjoint regions are uncorrelated, hence Gaussian independent:

$$\mathrm{Cov}(\eta_{uv}, \eta_{u'v'}) = \iint_{P_{uv}} \iint_{P_{u'v'}} \frac{\sigma^2\, \delta(\phi - \phi')\delta(\theta - \theta')}{A_{uv} A_{u'v'}}\, dA\, dA' = 0 \quad \Longrightarrow \quad \eta_{uv} \perp\!\!\!\perp \eta_{u'v'}. \tag{13}$$

A.5 Non-identical distribution

The variance of one pixel, using Eq. 10, Eq. 11, and Eq. 12, is

$$\mathrm{Var}(\eta_{uv}) = \frac{1}{A_{uv}^2} \iint_{P_{uv}} \iint_{P_{uv}} \sigma^2 \, \delta(\phi - \phi')\delta(\theta - \theta') \, dA \, dA' = \frac{\sigma^2}{A_{uv}} = \sigma^2 \, \frac{WH}{2\pi^2} \, \frac{1}{\sin\theta_v}. \quad (14)$$

Eq. 14 depends on the latitude index v through the factor $\sin\theta_v$. Pixels close to the poles ($\theta_v \approx 0$ or π) possess a larger variance than pixels near the equator ($\theta_v \approx \pi/2$). Hence

$$\mathrm{Var}(\eta_{uv}) \neq \mathrm{Var}(\eta_{u,v'}) \quad \text{for } v \neq v'.$$

B More Details on Method

Implementation Details. The sampling step for PAR is set to 64 and $r = 0.125$ by default. We use Janus Pro-7B to get the captions with the template as "Use one sentence to describe the photo in detail.". We then calculate the token lengths and keep them less than 77. Experiments shows that less than 0.1% of the captions do not meet the requirements, and we add "and briefly" at the end of those prompts.

Framework Details. The transformer takes patchified visual tokens (from the VAE encoder), masking indicators, and text embeddings as inputs. It outputs a conditional signal to drive the subsequent denoising network MLP. The decoding mechanism is illustrated in Fig. 9.

The MLP has multiple stacked blocks. Within each block, the input is first processed by AdaLNZero to get gating coefficients. It is then transformed using a projection layer consisting of two linear layers with silu activation. The result is then LN-normalized and multiplied by the gating coefficients, and finally combined with a residual connection.

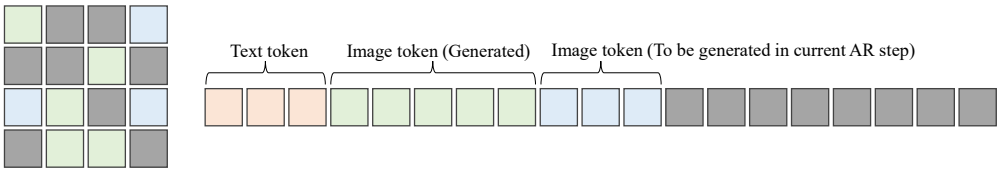

Figure 9: Illustration of decoding mechanism.

C More Empirical Studies and Visual Results

Time Analysis. It takes about 2 days to train the 1.4B model on 8 NVIDIA A100 GPUs. As shown in Tab. 4, we benchmark the inference speed for the 0.3B model with different AR steps using one NVIDIA A100 GPU with a batch size of 8. The denoising steps for MLP are 25.

Table 4: Ablations of inference time under different AR steps.

AR steps	16	32	64
Inference speed (sec/image) ↓	3.02	5.49	10.03

We also compare PAR-0.3B with PanFusion with 64 AR steps in Tab. 5.

Table 5: Comparison with PanFusion regarding inference time.

	PanFusion	PAR (ours)
Inference speed (sec/image) ↓	28.91	10.03
FID ↓	45.21	41.15

Table 6: Ablations of different padding ratios regarding inference time.

Padding Ratio	0	0.0625	0.125	0.25	0.5
Inference speed (sec/image) ↓	2.99	3.01	3.02	3.04	3.05
Additional costs	0	0.67%	1.00%	1.67%	2.01%

Table 7: Text-to-panorama results on the Matterport3D dataset.

	FAED ↓	FID ↓	CLIP Score ↑	DS ↓
DiffPano [70]	10.03	53.29	30.31	6.16
UniPano [40]	5.87	44.74	30.45	0.77
PAR-0.3B (ours)	3.39	41.15	30.21	0.58

As shown in Tab. 6, circular padding does not bring about additional computational cost in the transformer and MLP, which account for the majority of inference time. The AR step is 16.

More Results on Text-to-Panorama. Tab. 7 shows that our method has advantages on text-to-panorama task. We also provide more visual results in Fig. 10. Our model can generate reasonable panoramic images under the guidance of textual prompts. Tab. 9 provides ablation study for different denoising steps with our 0.3B model.

More Results on Panorama Outpainting. Tab. 8 shows that our method has advantages on panorama outpainting task. We provide more visual results for panorama outpainting in Fig. 11. We test the performance of our model in indoor setting and outdoor setting, and our model can achieve decent results, which proves its generalizability.

Visual Results of Circular Padding. Fig. 12 compares different circular padding strategies, including $r_{pre} = 0$ and $r_{pre} = 0.5$. r_{post} ranges from 0 to 0.5. It converges quickly with $r_{post} > 0$. r_{pre} helps to maintain cycle consistency at the semantic level.

Classifier-free Guidance. We evaluate PAR-1.4B with different CFG coefficients. The model obtains 40.04 FID when CFG=3 and 39.76 FID when CFG = 10, indicating that too large or too small guidance strength deteriorates the quality of the generation.

Ablations on other datasets. We include additional experiments using the Structured3D [78] dataset, which is a large-scale synthesized indoor dataset for house design with well-preserved poles. We sampled 9000 images for training and 1000 for testing. In Tab. 10, our method outperforms PanoLlama. Fig. 14 visualizes the synthesized results of PAR-0.3B. This indicates that the blur in the pole regions originates from the dataset and is irrelevant to the model, which can also be demonstrated by the visualizations of perspective projections in Fig. 13.

Zero-shot inference on OOD datasets. We evaluate panorama discontinuity using both our method and StitchDiffusion [61]. StitchDiffusion forces the model to fuse seam areas during inference. On the contrary, our pre-padding makes the model learn semantic consistency during the training phase, and post-padding achieves pixel-level consistency in the inference stage. In this experiment, PAR-0.3B and StitchDiffusion generate images for 100 text prompts sampled from a subset of SUN360, respectively. Our method achieves a DS score of 0.63, outperforming StitchDiffusion's 1.12.

For zero-shot outpainting, we compare the two methods on 100 images from the Structured3D dataset, which is excluded from both training sets for fairness. As shown in Tab. 11, our model outperforms Diffusion360.

Failure case. As shown in Fig. 15, our model may fail in some details of small objects, such as tables and sofas.

D Discussion

Comparisons to multi-view diffusion models. On the one hand, our AR-based method has several advantages over multi-view diffusion models (MVDMs). First, Computational Efficiency. MVDMs require generating several perspective images to cover a panorama, resulting in more computational

The image depicts a spacious, elegantly designed living room with large windows, white walls, and a mix of modern and traditional furniture, including sofas, a coffee table, and a grand piano.

The image depicts a spacious, elegant kitchen and dining area with a round wooden table, white chairs, and a large window adorned with curtains, showcasing a blend of modern and classic design elements.

The image depicts a spacious, well-lit living room with a mounted TV, comfortable seating, and a view of the kitchen and dining area in the background.

The image depicts a spacious, modern bathroom with a large bathtub, double vanity, and large windows allowing natural light to fill the room.

Figure 10: Visualization of text-to-panorama generation, including the generated results and corresponding textual prompts.

Table 8: Panorama outpainting results on the Matterport3D dataset.

	FID ↓	FID-h ↓
PanoDiff [62]	65.11	46.58
PAR w/o prompt	41.63	25.97

cost due to the attention mechanism. Second, Global Consistency. Coordinating multiple views demands complex attention mechanisms to ensure coherence, and struggles to maintain a consistent global understanding - sometimes leading to duplicated or inconsistent content. Third, Fewer Seam Issues. MVDMs must handle more seams at the boundaries between views, which increases the difficulty of achieving seamless stitching and can introduce visible artifacts.

On the other hand, since our model directly generates the entire panoramic image, it needs to use panoramic data to drive the pre-trained model (trained on perspective images) to adapt to the panoramic domain knowledge, which might be less efficient.

Broader Impacts. Our proposed PAR employs autoregressive set-by-set modeling for panoramic image generation tasks. It has significant advantages in generation performance compared with previous methods. Moreover, it shows the capability of zero-shot task generalization, like panorama outpainting and editing. This is an attempt towards the unification model in the field of panoramic image generation and will motivate people to explore the unification of different tasks in panorama generation. From the perspective of social impact, this will help the creation of artistic content, but at the same time it may result in the problem of fake content.

Safeguards. The content generated by the generative model, including AR models in this paper, demonstrates a high degree of correlation with the training data. From this perspective, it is important to ensure the fairness and cleanliness of the training data. In this way, we can effectively prevent the model from generating harmful content.

Limitations. We find that there is still a gap between the generated results and the real panoramic images, such as some details and textures. We argue that scaling on more realistic images can help alleviate this problem. However, due to the scarcity of panoramic data, we leave it as future work.

Table 9: Ablations of denoising steps.

Steps	10	20	30	40
FID ↓	41.57	40.19	41.98	43.77

Figure 11: Visualization of panorama outpainting results.

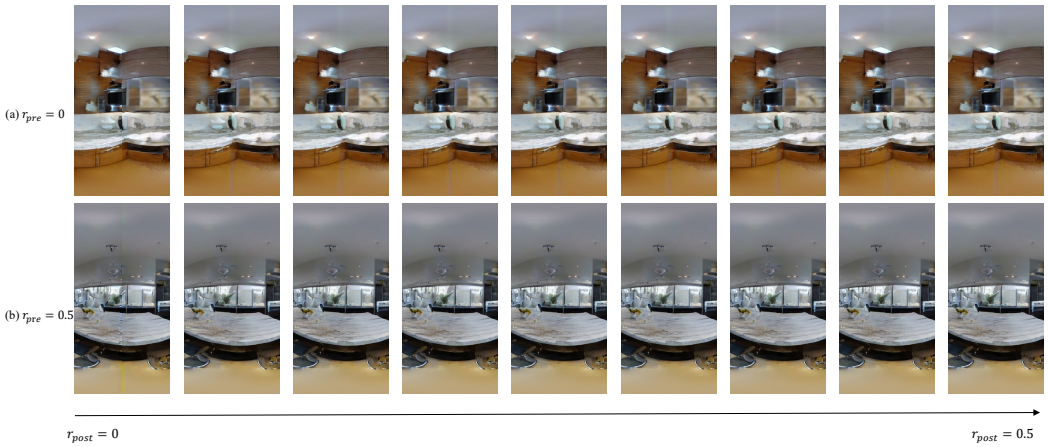

Figure 12: Visualization results of circular padding under different settings.

Table 10: Comparisons of PAR-0.3B and PanoLlama on Structured3D dataset.

	FID ↓	CLIP Score ↑	DS ↓
PanoLlama [80]	125.35	33.90	16.37
PAR-0.3B	47.02	30.75	0.68

Table 11: Zero-shot panorama outpainting results.

	FID ↓	FID-h ↓
Diffusion360 [18]	140.91	74.89
PAR w/o prompt	127.01	68.27

Panoramic Images Perspective Images

Figure 13: Perspective projections of synthesized results on Matterport3D dataset.

The image depicts a modern, well-lit interior of a home with a kitchen, dining area, hallway, living room, and staircase, showcasing a warm and inviting atmosphere.

The image depicts a modern, well-organized bedroom with a large bed, wooden flooring, and a variety of furniture including a wardrobe, a chair, a desk, and a dresser.

Figure 14: Visualizations of synthesized results on Structured3D dataset.

(a) The photo depicts a spacious, modern bedroom with a large bed, a sitting area, and a balcony overlooking a scenic view of the ocean.

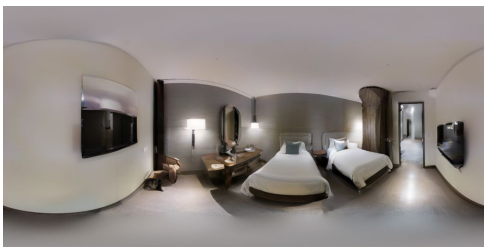

(b) The image depicts a modern, spacious hotel room with two twin beds, sleek furniture, and a clean, neutral color palette.

Figure 15: Failure cases.